NIH Public Access
Author Manuscript
Science. Author manuscript; available in PMC 2011 August 19.

Published in final edited form as:
Science. 2008 April 11; 320(5873): 233–236. doi:10.1126/science.1153758.

Segregation of Axial Motor and Sensory Pathways via Heterotypic Trans-Axonal Signaling

Benjamin W. Gallarda[1,*], **Dario Bonanomi**[1,*], **Daniel Müller**[2,3,*], **Arthur Brown**[4], **William A. Alaynick**[1], **Shane E. Andrews**[1], **Greg Lemke**[5], **Samuel L. Pfaff**[1,†], and **Till Marquardt**[2,3,†]

[1]Gene Expression Laboratory, Salk Institute for Biological Studies, 10010 North Torrey Pines Road, La Jolla, CA 92037, USA

[2]Developmental Neurobiology Laboratory, European Neuroscience Institute Göttingen, Max Planck Society/University Medical School Göttingen, Grisebachstrasse 5, 37077 Göttingen, Germany

[3]Deutsche Forschungsgemeinschaft Emmy Noether Group, European Neuroscience Institute Göttingen, Grisebachstrasse 5, 37077 Göttingen, Germany

[4]Biotherapeutics Research Group, Robarts Research Institute, Department of Anatomy and Cell Biology, University of Western Ontario, 100 Perth Drive, London, Ontario N6A 5K8, Canada

[5]Molecular Neurobiology Laboratory, Salk Institute for Biological Studies, 10010 North Torrey Pines Road, La Jolla, CA 92037, USA

Abstract

Execution of motor behaviors relies on circuitries effectively integrating immediate sensory feedback to efferent pathways controlling muscle activity. It remains unclear how, during neuromuscular circuit assembly, sensory and motor projections become incorporated into tightly coordinated, yet functionally separate pathways. We report that, within axial nerves, establishment of discrete afferent and efferent pathways depends on coordinate signaling between coextending sensory and motor projections. These heterotypic axon-axon interactions require motor axonal EphA3/EphA4 receptor tyrosine kinases activated by cognate sensory axonal ephrin-A ligands. Genetic elimination of trans-axonal ephrin-A → EphA signaling in mice triggers drastic motor-sensory miswiring, culminating in functional efferents within proximal afferent pathways. Effective assembly of a key circuit underlying motor behaviors thus critically depends on trans-axonal signaling interactions resolving motor and sensory projections into discrete pathways.

During neuromuscular circuit assembly, spinal motor neurons and dorsal root ganglion (DRG) sensory neurons coextend axons en route to peripheral targets, such as muscle and dermis (1, 2). Their close proximity and eventual pooling into common nerves prompts the question of how sensory and motor projections become organized into tightly coordinated, yet functionally separate afferent and efferent pathways. In chick embryos, peripheral

Copyright 2008 by the American Association for the Advancement of Science; all rights reserved.

†To whom correspondence should be addressed. till.marquardt@mpi-mail.mpg.de (T.M.); pfaff@salk.edu (S.L.P.).
*These authors contributed equally to this work.

Supporting Online Material
www.sciencemag.org/cgi/content/full/320/5873/233/DC1
Materials and Methods
Figs. S1 to S7
Table S1
References
Movies S1 to S4

NIH-PA Author Manuscript
NIH-PA Author Manuscript
NIH-PA Author Manuscript

NIH-PA Author Manuscript

NIH-PA Author Manuscript

NIH-PA Author Manuscript

sensory-motor trajectories become rapidly organized into defined mutually exclusive intranerve fascicles (3). This early appearance of discrete intranerve trajectories suggests that trans-axonal interactions might drive the segregation (3, 4). Axon-axon interactions have been implicated in olfactory and retinal axon targeting in *Drosophila* and mouse (5–7) and also in chick lateral motor column (LMC) and sensory axon sorting, respectively (8, 9). Moreover, embryological studies suggest that trans-axonal interactions impart vital cues for proper navigation of proprioceptive sensory axons (4, 10). The nature of such interactions and their contribution to neuromuscular circuit assembly, however, remain unclear (11).

To study the mechanisms underlying the establishment of discrete peripheral nerve pathways, we first analyzed the relative behavior of identified motor and sensory projections during neuromuscular development (12). We generated mice carrying ventral motor neuron–specific *Hb9::eGFP* (13) and previously generated sensory neuron-targeted *Brn3a::tau:lacZ* transgenes (14). In proximal peripheral nerves of *Hb9::eGFP;Brn3a::tau:lacZ* embryos, sensory and motor projections segregate into discrete $eGFP^+$ (where eGFP is enhanced green fluorescent protein) and tau:βGal^+ (where βGal is β-galactosidase) fascicles (Fig. 1, A to C and F). This pattern emerges after sensory axons join motor projections at the dorsal root–ventral root (DR-VR) junction (Fig. 1, A to C, and fig. S1) and precedes the stages of Schwann cell precursor invasion (Fig. 1, A to C; Fig. 2, A to C; and fig. S1) (15). In most cases, sensory projections trail earlier-extending motor axons (Fig. 1D and fig. S1, A to C and J to K) (1). However, median medial motor column (MMCm) axons extend toward axial targets with a delay that results in a much closer association with pioneering sensory axons in the dorsal ramus pathway (Fig. 1E and fig. S1, D to I and L to M) (16). The initial interactions between MMCm and DRG neurites eventually resolve into sharply segregated proximal motor-sensory pathways (Fig. 1, A to C and F, and fig. S1K). These observations suggest that, particularly within axial nerves, axon type-segregated patterns may emerge through interactions among coextending motor and sensory projections.

To address this possibility, we established an assay to study the interactions between axial motor and sensory projections in vitro (Fig. 1G and fig. S2) [see supporting online material (SOM)]. After extended co-culture periods, axial motor and sensory axons became organized into almost completely exclusive but parallel sensory and motor trajectories (Fig. 1, H to J, and fig. S3, A and M to N)—a pattern remarkably reminiscent of the aligned but discrete efferent and afferent pathways observed in situ (Fig. 1, A to C and F). Using nerve growth factor (NGF) and neurotrophin-3 to select for nocioceptive and proprioceptive classes of sensory neurons, respectively, we found that effective segregation of sensory and motor projections occurred irrespective of sensory subtype. Nevertheless, MMCm axons more frequently crossed into proprioceptive explants compared with nocioceptive cultures (fig. S2, F to K). Homotypic (e.g., motor-motor) co-cultures failed to display axon segregation, stressing the heterotypic nature of the underlying interactions (Fig. 1, K to L).

To address the cellular basis for these interactions, we monitored live co-cultured axial motor and sensory axons (fig. S3, C to L, and movies S1 and S2). Acute encounters of motor axons with sensory processes triggered repulsive growth-cone behaviors, including wholesale collapse followed by partial axon retraction (11.7%, $n = 51$ growth-cone encounters) (fig. S3, B and C to G, and movie S2). Heterotypic encounters, however, more frequently elicited intermittent retraction of filopodial and lamelli-podial processes, followed by motor growth-cone reorientation parallel to sensory axon trajectories (70.5%, $n = 51$) (fig. S3, H to L; movie S1; and table S1). Homotypic encounters between either intersecting motor or sensory axons, in contrast, failed to evoke repulsive behaviors, allowing largely unhindered crossings of axons (2.3% total motor growth-cone repulsion, $n = 43$, versus 82.3% heterotypic repulsion, $n = 51$) (Fig. 1, K to L; movie S3; and table S1). These observations raise the possibility that the sorting of axial motor and sensory

NIH-PA Author Manuscript

NIH-PA Author Manuscript

NIH-PA Author Manuscript

projections into separate intranerve pathways is achieved through heterotypic contact-dependent repulsive interactions.

What are the mechanisms underlying heterotypic motor-sensory segregation? Among several candidate molecules, we focused on the EphA family of receptor tyrosine kinases and their cognate cell surface–linked glycosylphosphatidylinositol-anchored ephrin-A ligands, whose distribution is consistent with a role in trans-signaling between motor and sensory axons (17, 18). When engaged by ephrin-As, EphAs typically trigger contact-dependent repulsion, which has been shown to drive diverse aspects of central nervous system development and plasticity (5, 19). DRG sensory neurons and their peripheral processes express high levels of ephrin-A protein (Fig. 2, D to F, and fig. S4, B, F to G, K, and N), consistent with the reported *ephrin-A2* and *ephrin-A5* mRNA expression in DRGs (17, 20). Conversely, high levels of both EphA3 and EphA4 are detected on MMCm axons (Fig. 2, G to I; fig. S4, C, H to I, L, and O; and fig. S6, A to D). Likewise, EphA4 (but not EphA3) is also expressed on LMC axons (17, 18, 20, 21). The complementary distribution of EphAs and ephrin-As on MMCm and sensory axons thus mirrors the segregation of axonal processes within proximal nerves.

To address the potential role of signaling between sensory ephrin-As and motor axonal EphAs, we first examined the impact of eliminating EphA receptors from motor neurons on interaxonal segregation in vivo. To tackle potential redundant functions shared by different EphAs, we generated mice carrying targeted null mutations for both *EphA3* (18) and *EphA4* (21) to obtain *EphA3/EphA4*-deficient (*EphA3*$^{-/-}$;*EphA4*$^{-/-}$) animals. Subsequent intercrossing with *Hb9::eGFP* facilitated selective analysis of motor axon behavior upon EphA removal in *EphA3*$^{-/-}$;*EphA4*$^{-/-}$;*Hb9::eGFP* embryos. The loss of either *EphA3* or *EphA4* alone did not trigger overt defects in motor-sensory organization, although *EphA4*$^{-/-}$ mutants displayed marked peroneal-nerve thinning, consistent with the well-established role of EphA4 in dorsal-ventral LMC axon routing in the limb (21, 22). However, the successive loss of wild-type (WT) *EphA3* and *EphA4* alleles in either *EphA4* or *EphA3* null backgrounds, respectively, resulted in the cumulative misrouting of motor axons into DRGs (Fig. 2, L to M; Fig. 3, D to E; and fig. S5, A to F). *EphA3/EphA4* double-null mutants displayed marked ectopic invasion of motor axons into DRGs at all rostro-caudal levels (Fig. 2, L to M, and fig. S4, A to F). Retrograde neuronal tracing experiments revealed that the motor axons entering the DRG originated from axial motor neurons normally coexpressing EphA3 and EphA4, but not from other motor neuron subtypes (fig. S6, A to D). Despite drastic changes in axial motor projections, sensory axons retain normal segregation from motor trajectories in *EphA3/EphA4* mutants (fig. S6, I to T)—indicating the cell-autonomous action of motor axonal EphAs in establishing discrete proximal motor and sensory trajectories.

We next generated *EphA3*$^{-/-}$;*EphA4*$^{-/-}$; *Hb9::eGFP;Brn3a::tau:lacZ* mice, allowing the simultaneous visualization of motor and sensory axons at high resolution in EphA-deficient backgrounds. The examination of the intranerve segregation pattern *EphA3*$^{-/-}$;*EphA4*$^{-/-}$;*Hb9::eGFP; Brn3a::tau:lacZ* embryos revealed that misrouted axial motor axons entered proximal sensory pathways after initially following proper VR trajectories (Fig. 2, O to P, and fig. S5, G to I). Upon reaching the DR-VR junction, however, these motor axons fanned out into proximal sensory pathways before entering the DRG proper (Fig. 2, O to P, and fig. S5, G to N). The elimination of *EphA3* and *EphA4* from axial motor neurons thus resulted in the extensive intermingling of motor and sensory projections within proximal peripheral nerves (Fig. 2, Q to T), yet this did not lead to defasciculation outside peripheral nerve pathways (Fig. 2P and fig. S5, E to I). In contrast, distal nerve segments supplied by nonaxial motor columns innervating thorax and limb muscles maintained largely normal motor-sensory intra-nerve patterns (fig. S6, I to Z). Thus,

NIH-PA Author Manuscript

NIH-PA Author Manuscript

NIH-PA Author Manuscript

with decreasing EphA receptor activity, axial motor axons become progressively capable of invading proximal sensory pathways.

Spinal motor neurons are embedded within local neural circuitries that determine stereotypic patterns of activity (23, 24), raising the question of whether ectopic motor projections sustained within sensory pathways would display normal activity patterns (fig. S7, D and E). To address this, we performed electrophysiological recordings from DRs and VRs in perinatal *EphA3/EphA4*-deficient and control animals. In these preparations, central pattern generator (CPG)–driven rhythmic motor activity was pharmacologically evoked and recorded with extracellular suction electrodes from lumbar VRs (Fig. 3, A to C, and fig. S7, A and B) (25). We reasoned that ectopic activity coupled to CPG-driven locomotor patterns, such as derived from MMCm neurons (26), would be detectable through recordings from DR central afferents (fig. S6, A and B).

EphA3/EphA4-deficient lumbar (L2) VRs displayed typical periodic activity bursts, reflecting CPG-coupled locomotor activity (Fig. 3, A to C) (23–25). In contrast, the activity recorded from DRs of WT and *EphA3/EphA4* single or double heterozygous animals was irregular, small in amplitude, and did not display significant rhythmicity (Fig. 3, A and F). This suggests that the normal segregation of proximal motor-sensory pathways effectively isolates the DR from exhibiting detectable locomotor activity. Even so, DRs of *EphA3/EphA4* double-null mutants showed strong amplitude activity bursts mirroring the rhythmicity of VR-derived motor activity (Fig. 3, C and F, and fig. S6C). Recordings performed on $EphA3^{+/-};EphA4^{-/-}$ DRs frequently revealed similar, albeit weaker and less regular, locomotor-like activity bursts (Fig. 4, B and F), consistent with the *EphA3/EphA4*-dose dependency of motor-sensory miswiring (Fig. 3, D to E, and fig. S5, A to F). Loss of *EphA3/EphA4* thus erodes the normal segregation pattern between axial motor neurons and DRG sensory neurons and results in MMCm projections within afferent pathways that maintain their functional coupling with spinal locomotor circuits.

The drastic proximal motor-sensory mis-wiring in *EphA3/EphA4* mutants suggests that these effects were due to a loss of trans-axonal ephrin-A → EphA signaling. To test this, we analyzed the impact of *EphA3*/*EphA4* elimination on the sensitivity of axial motor neurons toward increasing doses of exogenous recombinant ephrin-A protein in vitro (Fig. 4, A to E; fig. S2, A to E; and movie S4) (20). In this assay, *EphA3/EphA4*-deficient MMCm axons displayed a complete loss of sensitivity toward ephrin-A–induced growth-cone collapse (Fig. 4A). We next tested whether elimination of sensitivity toward ephrin-As would translate into a loss of motor growth-cone responsiveness toward repulsion by sensory axons. To this end, MMCm explants derived from $EphA3^{-/-};EphA4^{-/-};Hb9::eGFP$ or control embryos were co-cultured with stage-matched WT DRGs (Fig. 4, F to K). In this assay, *EphA3/EphA4*-deficient axial motor axons crossed over and intermingled with sensory trajectories that, in the control, were marked by two discrete sheets of parallel motor and sensory projections (Fig. 4, F to G, I, and J). Moreover, *EphA3/EphA4*-deficient motor axons frequently invaded co-cultured DRGs, mirroring motor-sensory misrouting defects in $EphA3^{-/-};EphA4^{-/-}$mutants in situ (Fig. 4, H and L). We further addressed whether cell-autonomous EphA-mediated activity is required in motor axons, or if some of the observed effects were due to non-cell–autonomous and/or pleiotrophic requirements, such as proper sensory neuron maturation. To investigate this, we co-cultured MMCm explants derived from WT embryos with DRGs derived from stage-matched *EphA3/EphA4*-deficient embryos. In these experiments, co-cultured motor and sensory projections organized into mutually exclusive parallel trajectories, demonstrating that *EphA3*/*EphA4* elimination does not affect the ability of DRG sensory axons to repel WT motor axons (Fig. 4, I to K and L). The loss of motor axonal EphA receptors thus leads to severely reduced sensitivity toward repulsion by sensory axons (Fig. 4L), consistent with an ephrin-A → EphA–mediated

NIH-PA Author Manuscript

NIH-PA Author Manuscript

NIH-PA Author Manuscript

repulsive signaling event that normally operates between adjacent axial motor axons and sensory projections.

Assembly of complex circuitries generating meaningful homeostatic, behavioral, or cognitive outputs necessarily entails the formation of concisely delineated neural pathways (27). This is highlighted by conditions abolishing segregation of normally discrete axonal pathways, including nerve injury–induced neuropathic pain (28). The present study provides evidence that, during neuromuscular circuit assembly, repulsive trans-axonal ephrin-A → EphA signaling contributes to the establishment of discrete peripheral afferent and efferent pathways. These interactions act at the level of newly extending axial motor growth cones and sensory neurites, effectively blocking efferent access to proximal afferent pathways. Our findings suggest that the heterotypic motor-sensory segregation diverges between axial and nonaxial motor neuron classes at two levels: (i) first, by means of relative outgrowth order favoring direct motor-sensory growth-cone encounter for late-extending axial over earlier nonaxial projections and (ii) second, through differential reliance on ephrin-A/EphA-dependent and -independent mechanisms. The mechanistic basis for the orderly segregation of nonaxial motor-sensory components remains to be identified. Apart from mechanisms driving axon targeting and synaptogensis, the finely tuned coordination between coextending, yet functionally distinct projection types may thus emerge as a key feature in the assembly of neural circuits in general.

Supplementary Material

Refer to Web version on PubMed Central for supplementary material.

Acknowledgments

We thank K. Lettieri and A. Klusowski for outstanding technical assistance, E. Turner for sharing *Brn3a::tau:lacZ* mice, and M. Goulding and A. Boyd for *EphA4* mice. T.M. was supported by the Deutsche Forschungsgemeinschaft Emmy Noether Program and Pioneer Foundation Awards. G.L. and S.L.P. were supported by National Institute of Neurological Disorders and Stroke grants NS031249-14A1 and NS054172-01A2.

References and Notes

1. Landmesser LT. Int J Dev Neurosci. 2001; 19:175. [PubMed: 11255031]
2. Chen HH, Hippenmeyer S, Arber S, Frank E. Curr Opin Neurobiol. 2003; 13:96. [PubMed: 12593987]
3. Honig MG, Frase PA, Camilli SJ. Development. 1998; 125:995. [PubMed: 9463346]
4. Landmesser L, Honig MG. Dev Biol. 1986; 118:511. [PubMed: 3792620]
5. Luo L, Flanagan JG. Neuron. 2007; 56:284. [PubMed: 17964246]
6. Feinstein P, Mombaerts P. Cell. 2004; 117:817. [PubMed: 15186781]
7. Brown A, et al. Cell. 2000; 102:77. [PubMed: 10929715]
8. Tang J, Rutishauser U, Landmesser L. Neuron. 1994; 13:405. [PubMed: 8060618]
9. Honig MG, Rutishauser US. Dev Biol. 1996; 175:325. [PubMed: 8626036]
10. Tosney KW, Hageman MS. J Exp Zool. 1989; 251:232. [PubMed: 2769202]
11. Wang G, Scott SA. Dev Biol. 1999; 208:324. [PubMed: 10191048]
12. Materials and methods are available as supporting material on *Science* Online.
13. Lee SK, Jurata LW, Funahashi J, Ruiz EC, Pfaff SL. Development. 2004; 131:3295. [PubMed: 15201216]
14. Quina LA, et al. J Neurosci. 2005; 25:11595. [PubMed: 16354917]
15. Dong Z, et al. J Neurosci Res. 1999; 56:334. [PubMed: 10340742]
16. Shirasaki R, Lewcock JW, Lettieri K, Pfaff SL. Neuron. 2006; 50:841. [PubMed: 16772167]
17. Iwamasa H, et al. Dev Growth Differ. 1999; 41:685. [PubMed: 10646798]

NIH-PA Author Manuscript

NIH-PA Author Manuscript

NIH-PA Author Manuscript

18. Vaidya A, Pniak A, Lemke G, Brown A. Mol Cell Biol. 2003; 23:8092. [PubMed: 14585969]
19. Klein R. Curr Opin Cell Biol. 2004; 16:580. [PubMed: 15363810]
20. Marquardt T, et al. Cell. 2005; 121:127. [PubMed: 15820684]
21. Helmbacher F, Schneider-Maunoury S, Topilko P, Tiret L, Charnay P. Development. 2000; 127:3313. [PubMed: 10887087]
22. Kramer ER, et al. Neuron. 2006; 50:35. [PubMed: 16600854]
23. Goulding M, Pfaff SL. Curr Opin Neurobiol. 2005; 15:14. [PubMed: 15721739]
24. Kiehn O. Annu Rev Neurosci. 2006; 29:279. [PubMed: 16776587]
25. Myers CP, et al. Neuron. 2005; 46:37. [PubMed: 15820692]
26. Gramsbergen A, Geisler HC, Taekema H, van Eykern LA. Brain Res Dev Brain Res. 1999; 112:217.
27. Eccles JC. Appl Neurophysiol. 1981; 44:5. [PubMed: 7294779]
28. McLachlan EM, Janig W, Devor M, Michaelis M. Nature. 1993; 363:543. [PubMed: 8505981]

NIH-PA Author Manuscript

NIH-PA Author Manuscript

NIH-PA Author Manuscript

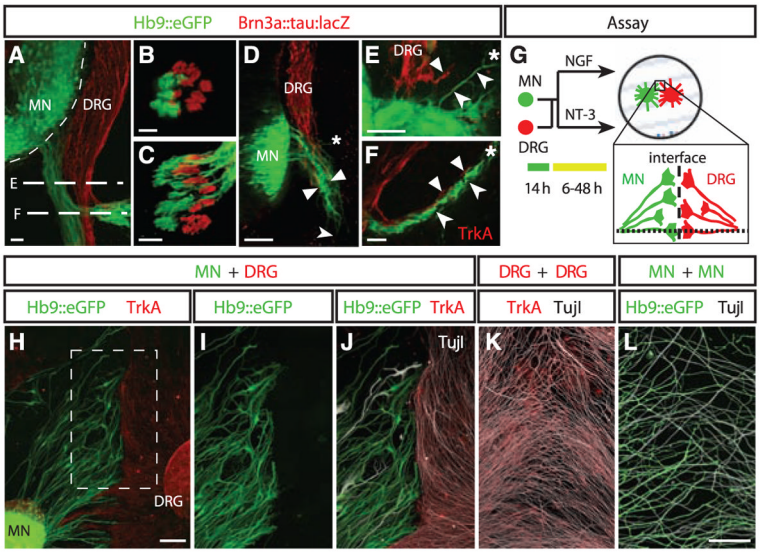

Fig. 1.

Spontaneous delineation of axial motor and sensory projections during neuromuscular circuit assembly. (**A**) 120-μm lumbar (L5 to L6) transversal E12.5 section at the DR-VR junction. eGFP, motor axons; anti-βGal, sensory axons (red); MN, motor neurons. (**B** and **C**) 120-μm nerve cross sections. Levels, dashed lines in (A). (C) MMCm projections through sensory fascicles. (**D** and **E**) 120-μm lumbar E10.0. Sequential advance: nonaxial motor axons, bottom arrowheads; sensory axons, top arrowheads. Asterisks denote emerging MMCm axons. (E) E10.0 dorsal ramus, emerging sensory; MMCm growth cone, top and bottom arrowheads. (**F**) E12.5 dorsal ramus, segregated sensory-motor pattern; TrkA, tropomyosin-related kinase A. (A to F) Scale bars, 20 μm. (**G**) Sensory-motor interaction assay (see SOM). MN and DRG explants. (**H** to **J**) Motor (green) and sensory (red) axons segregate in vitro. The dashed-line box indicates the enlarged area in (I) and (J); TujI, βIII-tubulin. (I and J) Axon interface of (H). (**K** and **L**) Absence of homotypic axon segregation. (H) Scale bar, 100 μm. (I to L) Scale bar, 100 μm.

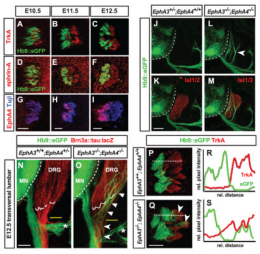

Fig. 2.

Loss of proximal motor-sensory segregation upon eliminating MMCm-expressed EphA receptors. (**A** to **I**) 60-to-120–μm L3 to L5 nerve cross sections: complementary distribution of EphA4 (anti-EphA4), ephrin-As (EphA3-Fc) in motor (eGFP), and sensory axons (TrkA). Scale bar, 25 μm. (**J** to **M**) 60-μm thoracic transversal. Scale bars, 100 μm. (K and L) No motor projections in DRG (Isl1/2: sensory nuclei). (L and M) MMCm axons misproject into DRG [arrowhead in (L)]. Dashed line indicates the spinal cord. (**N** and **O**) 180-μm transversal. (N) Control motor-sensory trajectories. (O) MMCm axons invade proximal sensory pathways and DRG (arrowheads). Solid lines indicate the DR-VR junction; asterisks denote the dorsal ramus; and dashed lines indicate motor and sensory somas. Scale bar, 50 μm. (**P** and **Q**) 120-μm T10 nerve cross. Dotted lines indicate line measurements in (R) and (S). (P) Control motor-sensory trajectories. (Q) Ectopic MMCm axons associate with sensory fascicles (arrowheads). Scale bar, 20 μm. (**R** and **S**) Intensity profiles of line measurements indicated in (P) and (Q).

NIH-PA Author Manuscript NIH-PA Author Manuscript NIH-PA Author Manuscript

NIH-PA Author Manuscript

NIH-PA Author Manuscript

NIH-PA Author Manuscript

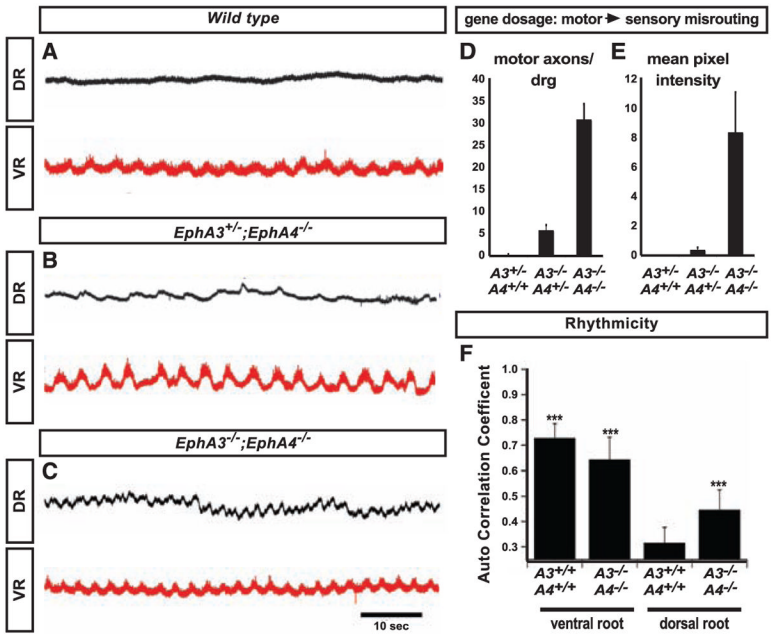

Fig. 3.

Axial motor axons within sensory pathways retain functional coupling with spinal locomotor circuits. (**A** to **C**) E18.5 DR recordings (top). Genotype-matched VR traces (bottom). Locomotor activity evoked by 10 μM *N*-methyl D,L-aspartate (NMA) and 20 μM serotonin [5-hydroxytryptamine (5-HT)]. (A) No rhythmic activity in WT DR, rhythmic activity in VR. (B) Some DR activity. (C) Strong rhythmic DR activity. (**D** and **E**) Quantitative summary: motor-sensory misrouting (see SOM and fig. S5, A to C). *EphA3*$^{+/-}$;*EphA4*$^{-/-}$ (*n* = 6 spinal cords), *EphA3*$^{-/-}$;*EphA4*$^{+/-}$ (*n* = 8), *EphA3*$^{-/-}$;*EphA4*$^{-/-}$ (*n* = 6). Error bars indicate SD. (**F**) Autocorrelation analysis. Significance: WT, *EphA3/EphA4*-deficient VRs ($P < 0.001$, each); WT DR ($P > 0.05$), *EphA3/EphA4*-deficient DR ($P < 0.001$). WT (*n* = 6), *EphA3/EphA4*-deficient (*n* = 6). Asterisks denote significance; error bars indicate SD.

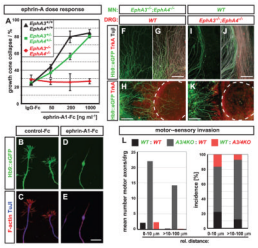

Fig. 4.

Motor axonal EphAs impose sensitivity toward sensory-expressed ephrin-As. (**A**) *EphA3/EphA4* deficiency abolishes ephrin-A–induced MMCm growth-cone collapse in vitro. IgG, immunoglobulin G. (**B** to **E**) Example of control-Fc (B and C) and ephrin-A1–Fc (D and E) stimulation. Typical Hb9::eGFP^{+} MMCm growth cones (B and C); ephrin-A1–Fc triggers collapse to filopodialike thread, F-actin^{+}TujI^{+} swelling. Scale bar, 10 μm. (**F** to **K**) Autonomous *EphA3/EphA4* requirement in MMCm axons for repulsion by sensory axons. Scale bars, 100 μm. (F and G) *EphA3/EphA4*-deficient MMCm axons extensively cross WT sensory axons and (H) invade WT DRGs (dashed outline). (I and J) *EphA3/EphA4* null sensory axons repel WT MMCm axons. (K) No WT motor axon invasion of *EphA3/EphA4* null DRG. (**L**) Quantitative summary. Mean number of invasion events per DRG (left); stacked column diagram represents percent invaded DRGs per genotype (right). Explant combinations are indicated. Relative distance is between motor-sensory explants.

NIH-PA Author Manuscript NIH-PA Author Manuscript NIH-PA Author Manuscript